



HAL
open science

Structure and function of SirC from *Bacillus megaterium* - a metal binding precorrin-2 dehydrogenase

Heidi L Schubert, Ruth S Rose, Helen K Leech, Amanda A Brindley,
Christopher P Hill, Stephen E. J. Rigby, Martin J Warren

► To cite this version:

Heidi L Schubert, Ruth S Rose, Helen K Leech, Amanda A Brindley, Christopher P Hill, et al..
Structure and function of SirC from *Bacillus megaterium* - a metal binding precorrin-2 dehydrogenase.
Biochemical Journal, 2008, 415 (2), pp.257-263. 10.1042/BJ20080785 . hal-00479012

HAL Id: hal-00479012

<https://hal.science/hal-00479012>

Submitted on 30 Apr 2010

HAL is a multi-disciplinary open access archive for the deposit and dissemination of scientific research documents, whether they are published or not. The documents may come from teaching and research institutions in France or abroad, or from public or private research centers.

L'archive ouverte pluridisciplinaire **HAL**, est destinée au dépôt et à la diffusion de documents scientifiques de niveau recherche, publiés ou non, émanant des établissements d'enseignement et de recherche français ou étrangers, des laboratoires publics ou privés.

Structure and function of SirC from *Bacillus megaterium* - a metal binding precorrin-2 dehydrogenase

Heidi L. Schubert*, Ruth S. Rose†, Helen K. Leech†, Amanda A. Brindley†, Christopher P. Hill*, Stephen E. J. Rigby‡ and Martin J. Warren†

* Department of Biochemistry, University of Utah, Salt Lake City, UT 84112; USA

† UK Protein Sciences Group, Department of Biosciences, University of Kent, Canterbury, Kent CT2 7NJ, UK

‡ School of Biological and Chemical Sciences, Queen Mary, University of London, Mile End Road, London E1 4NS

Short running title: structure of a precorrin-2 dehydrogenase

Abbreviations: S-adenosyl-L-methionine, SAM

Correspondence to either:

M. J. Warren, tel 00 44 1227 824690, email: m.j.warren@kent.ac.uk

or

H. L. Schubert, tel 00 1 801-585 9776, email: heidi@biochem.utah.edu

Key words: precorrin-2, sirohydrochlorin, siroheme, cobalamin (vitamin B₁₂), dehydrogenase, chelatase

SYNOPSIS.

In *Bacillus megaterium*, the synthesis of vitamin B₁₂ (cobalamin) and siroheme diverge at sirohydrochlorin along the branched modified tetrapyrrole biosynthetic pathway. This key intermediate is made by the action of SirC, a precorrin-2 dehydrogenase that requires NAD⁺ as a cofactor. The structure of SirC has now been solved by X-ray crystallography to 2.8 Å resolution. The protein is shown to consist of three domains and has a similar topology to the multifunctional siroheme synthases Met8p and the N-terminal region of CysG, both of which catalyse not only the dehydrogenation of precorrin-2 but also the ferrocyclization of sirohydrochlorin to give siroheme. Guided by the structure, a number of active site residues within SirC were investigated by site-directed mutagenesis. No active site general base was identified, although surprisingly some of the resulting protein variants were found to have significantly enhanced catalytic activity. Unexpectedly, SirC was found to bind metal ions such as cobalt and copper, and to bind them in an identical fashion to that observed in Met8p. It is suggested that SirC may have evolved from a Met8p-like protein by loss of its chelatase activity. It is proposed that the ability of SirC to act as a single monofunctional enzyme, in conjunction with an independent chelatase, may provide greater control over the intermediate at this branchpoint in the synthesis of siroheme and cobalamin.

INTRODUCTION

Siroheme is a modified tetrapyrrole that is required as a prosthetic group in the six electron reduction of both sulfite and nitrite [1-4]. As with all modified tetrapyrroles, siroheme is synthesized via a branched biosynthetic pathway that also oversees the construction of molecules such as heme and cobalamin (vitamin B₁₂) [5, 6]. The first macrocyclic and branchpoint precursor in the pathway is uroporphyrinogen III. In the Bacilli, siroheme is synthesized from uroporphyrinogen III in three steps (Figure 1) [7, 8]. This transformation is initiated by the addition of two S-adenosyl-L-methionine (SAM) derived methyl groups to positions 2 and 7 of the uroporphyrinogen III framework in a reaction catalyzed by SirA (S-adenosyl-L-methionine uroporphyrinogen III methyltransferase, SUMT, 2.1.1.107) to generate precorrin-2 [8]. Subsequently, this highly unstable dipyrrocorphin [9] is dehydrogenated by SirC (precorrin-2 dehydrogenase, 1.3.1.76) in an NAD⁺-dependent process to yield sirohydrochlorin [8]. Finally, ferrochelation by SirB (sirohydrochlorin ferrochelatase, 4.99.1.4) yields the end product siroheme [8], which is duly incorporated into either the appropriate assimilatory sulfite or nitrite reductase.

Sirohydrochlorin also acts as an intermediate in cobalamin biosynthesis, where cobalt insertion by enzymes such as CbiK [10, 11] or CbiX [5, 12] ensures that the intermediate is further manipulated along the anaerobic cobalamin biosynthesis branch of the pathway (Figure 1) [5]. In this respect, SirC plays an important role in both siroheme and cobalamin biosynthesis [8].

In *Saccharomyces cerevisiae*, the transformation of uroporphyrinogen III into siroheme requires just two enzymes, a methyltransferase (Met1p) for the synthesis of precorrin-2, and a bifunctional dehydrogenase/ferrochelatase (Met8p) (Figure 1) [13, 14]. The sequence of the bifunctional Met8p displays similarity to the monofunctional SirC and thus Met8p would appear to be a dehydrogenase that has acquired chelatase activity [8]. Met8p has been crystallized and the structure of the enzyme solved to 2.2 Å resolution [15], revealing that the protein adopts a novel fold that bears no resemblance to the previously determined structures of cobalto- [10, 16] or ferrochelataases [17, 18]. Analysis of mutant variants of Met8p suggests that the catalytic activities are accommodated within a single active site, and that Asp141 plays an essential role in both dehydrogenase and chelatase processes [15].

In some bacteria, the transformation of uroporphyrinogen III into siroheme is mediated by a single multifunctional enzyme called CysG (Figure 1) [19, 20]. In effect, CysG represents a fusion between a uroporphyrinogen III methyltransferase and a bifunctional dehydrogenase/ferrochelatase (such as Met8p). This interpretation has been confirmed by gene dissection and mutagenesis experiments that indicate that the N-terminal 200 amino acids of CysG house the dehydrogenase/ferrochelatase functionality whereas the C-terminal 257 amino acids mediate the methyltransferase activity [21]. It has been assumed that the bifunctional catalytic activities found associated with Met8p and the N-terminal region of CysG have arisen by acquisition of metal binding and metal insertion activity into the pre-existing framework of the dehydrogenase [8]. The recent structure elucidation of CysG also revealed that the enzyme is a phosphoprotein, where phosphorylation of serine 220 appears to control the activity of the enzyme [22]. A driving force for the appearance of the multifunctional enzymes could be to direct substrate channelling along a particular branch of the pathway. This would explain why Bacilli have separate enzymes for the siroheme branch since it allows sirohydrochlorin to be used not only for siroheme synthesis but also for cobalamin production.

Structure of a precorrin-2 dehydrogenase

In this paper we report on the structure and function of the *Bacillus megaterium* SirC, an NAD⁺-dependent precorrin-2 dehydrogenase, and compare it to the structure of Met8p, which is both a dehydrogenase and sirohydrochlorin ferrochelataase. In contrast to the previous idea that Met8p may have arisen from a precorrin-2 dehydrogenase by acquisition of chelataase activity, we suggest that SirC is more likely to have evolved from a protein such as Met8p by loss of its chelataase activity.

Stage 2(a) POST-PRINT

THIS IS NOT THE FINAL VERSION - see doi:10.1042/BJ20080785

EXPERIMENTAL

Chemicals and reagents: Chemicals and reagents were purchased from Sigma-Aldrich Ltd unless otherwise stated. Bacterial strains were purchased from Novagen, Invitrogen or Promega.

Protein purification: SirC was produced recombinantly in *Escherichia coli* as described previously [8]. Briefly, *sirC* was cloned into pET14b and transformed into BL21(DE3)pLysS(codon+) cells. Upon induction with IPTG (0.4 mM), SirC was produced with a N-terminal hexa-histidine tag. The protein was purified using a Ni²⁺ chelating column followed by dialysis into 20 mM sodium Citrate, pH 6.5, 100 mM NaCl, 1mM DTT and size exclusion chromatography. Met8p was purified as described previously [15].

Mutagenesis: The SirC mutants, Asn98Ala, Ser101Ala, Ser101Asp, Ser102Ala, Asp105Ala and Ser124Ala were generated using the Stratagene site-directed mutagenesis QuikChange kit, by following the manufacturer's instructions.

Precorrin-2 dehydrogenase assay: The assay was performed as described previously [15]. Briefly, activity was monitored by incubating precorrin-2 (2.5 μM) with 10 μg of SirC in a reaction volume of 1 ml with 7.5 mM NAD⁺ in 0.05 M Tris buffer, pH 8.0, containing 0.1 M NaCl. Sirohydrochlorin was monitored by the appearance of an absorption peak at 376 nm. Initial rates were recorded on a Hewlett Packard 8452A photodiode array spectrophotometer and assays were performed in triplicate.

Crystallization: The protein was concentrated to 8 mg/ml for crystallization trials. Crystals of SirC were grown by the vapour diffusion method using a hanging drop containing 2 μl of protein (8-10 mg/ml) and 2 μl of well solution composed 2.3 M (NH₃)₄SO₄, 0.1 M MES, 0.5–5 mM LiCl, pH 6.0. Potassium tetrachloroplatinate(II) and thimerisol derivatives were generated by soaking crystals for 5-10 minutes with 1 mM concentrations of metal compound in the well solution. All crystals were cryoprotected by elevating the solution around the crystal to 4 M (NH₃)₄SO₄ plus buffer and salt. All data were collected on a copper rotating anode X-ray source using CuKα radiation at 1.54 Å (4.5 kW, 100 mA), and processed with the HKL2000 suite [23].

Structure determination: The structure was determined to 2.8 Å by multiple isomorphous replacement with anomalous scattering using K₂PtCl₄ and thimerisol derivatives [24] (Table 1). Solvent flattening (solvent content of 50%) in RESOLVE [25] and subsequent automated model building generated a starting model. The model building was finished using the programs O [26] and Coot [27], CCP4 [28] and refinement in REFMAC [29] using TLS restraints generated a final model with an R_{factor} = 19.6% and R_{free} = 26.3%.

EPR: To produce samples of SirC for EPR spectroscopy, the protein was purified by metal chelate chromatography and cleaved by thrombin to remove the His-tag. The protein was purified further by size exclusion chromatography, as described above. The protein was taken into an anaerobic environment and exchanged into degassed buffer containing 50 mM HEPES, pH 8.0. The protein concentration was calculated as 47 μM on the basis of absorbance at 280 nm, from which EPR samples were generated containing 1:1 ratios of protein to Cu(II) or Co(II). The samples were sealed and frozen in liquid nitrogen. EPR spectra were obtained using a Bruker ELEXSYS E500/580 EPR spectrometer operating at X-band. Temperature control was effected using Oxford Instruments ESR900 and ESR935

Structure of a precorrin-2 dehydrogenase

cryostats interfaced with an ITC503 temperature controller. Experimental conditions were as given in the relevant figure captions.

Stage 2(a) POST-PRINT

THIS IS NOT THE FINAL VERSION - see doi:10.1042/BJ20080785

RESULTS AND DISCUSSION

Structure of SirC. The crystal structure of His-tagged *B. megaterium* SirC was determined by isomorphous replacement with anomalous scattering, and refined to R/R-free values of 19.5/26.3 with good geometry (Table I). The SirC structure comprises three domains: an N-terminal NAD⁺-binding domain, a central dimerization domain, and a C-terminal helical domain of unknown function (Figure 2). The structure resembles both the yeast siroheme synthase, Met8p (pdb code:1KYQ), with which it shares 11% identity, and the *Salmonella enterica* CysG (pdb code:1PJS), with which it shares 25% sequence identity over the N-terminal region of the protein. SirC is the smallest of these three enzymes by virtue of its shorter loops and secondary structure elements. All three of the proteins are homodimers, in which the three domains cross each other in the form of an “X” along a two-fold axis of symmetry. The orientation of the paired NAD⁺-domains is almost perpendicular to that of the paired helical domains.

Optimized alignments between dimeric SirC, CysG and Met8p over their first ~190 residues gives root mean square (rms) deviations of 3.0 – 4.8 Å, with the two bacterial proteins aligning more closely with each other than with the yeast Met8p structure. If NAD⁺-binding domains alone are aligned, the rms deviation between CysG and SirC is 1.1 Å over 100 Cα's. When monomers from each structure are aligned on their NAD⁺ binding domains, a significant relative twist in the orientation of the C-terminal helical domains is revealed (Figure 3). The structural deviation begins immediately after the NAD⁺ binding domain where the β-strands in the dimerization domain twist with respect to the two-fold axis of the homodimer but also a tilt away from the central core of the dimer.

Dehydrogenase active site. The NAD⁺-dependent dehydrogenase active site lies between the NAD⁺-domain, and the dimerization domain. The NAD⁺-binding site is empty in the SirC structure, though the high level of similarity with other NAD⁺-binding domains [30], and with the NAD⁺-bound structures of Met8p and CysG, facilitates the modelling of an NAD⁺ molecule to SirC (Figure 4). Canonical NAD⁺-binding domains contain two Rossmann folds where the adenosine portion of the NAD⁺ binds above the first β-strand, the phosphates sit on top of an invariant Gly-Gly-Gly sequence, and the nicotinamide portion of the coenzyme points toward the active site cleft. The NAD⁺-bound structures of Met8p and CysG have poorly defined electron density for the nicotinamide portion of the ligand, which is seen to adopt a variety of conformations in other related structures. We are therefore reasonably confident about the model presented here for the SirC-bound NAD⁺ adenine and phosphates, but more tentative in our suggestion that the nicotinamide resembles that of the Met8p-bound NAD⁺ and forms an edge of the putative active site cleft, rather than that of the CysG-NAD⁺ where the β-nicotinamide is located further away from the cleft.

A comparison of precorrin-2 dehydrogenase primary sequences from 18 species, all with greater than 55% identity to *B. megaterium* SirC, provides a list of nine invariant residues (data not shown). Due to the low overall sequence similarity, a combination of structure-based and amino acid sequence-based alignments is necessary to obtain an accurate alignment of the precorrin-2 dehydrogenase family. A limited sequence alignment paired with the SirC secondary structure is found in Figure 2c.

The active site cleft contains all of the invariant residues. Gly17, Gly18, and Gly19 lie within the NAD⁺-binding pocket, while the other seven invariant residues are predicted to interact with the precorrin-2 substrate. Asn98 lies at the base of the binding pocket pointing up toward

Structure of a precorrin-2 dehydrogenase

the open cleft (Figure 4). Ser124, Gly127, Ser129, and Pro130 (SxxGxSP) form a cluster of invariant residues on the opposite side of the active site cleft from the NAD⁺, within the central dimerization domain. Finally, Arg159 resides on the C-terminal helical domain and contributes to the active site from the alternate molecule of the homodimer.

Differences in the relative positions of the domains found in SirC, Met8p and the N-terminal region of CysG are clear (Figure 4) but the significance of these differences in terms of catalytic mechanism is unclear. Curiously, the location of the invariant Arg159 with respect to the active sites differs dramatically; it is clearly positioned within the active site cleft of SirC (Figure 4), whereas in the Met8p and CysG structures it is found 8-11 Å away from the active site. Sequence similarity is quite low in the C-terminal helical domain and Arg159 is only identified as an invariant residue after using secondary structural alignments of the three proteins (Figure 2c).

Modelling of a precorrin-2 substrate and site directed mutagenesis. We have built a plausible model of precorrin-2 bound to the active site cleft between the β-nicotinamide moiety and the cluster of invariant residues (Figure 4). The bond between C14 and C15 is oxidized during the dehydrogenase reaction with a concomitant loss of the proton from the C-ring pyrrole N3. The modelled precorrin-2 substrate places the C15 atom nearest to the β-nicotinamide while pointing the A- and B-rings toward the SxxGxSP residue cluster (Figure 4). In this position, the methylated A- and B-rings pack against conserved residues in the dimerization domain, and their acetate and propionate side chains extend further into the cleft where they could form hydrogen bonds with the main chain carbonyl oxygens and amide nitrogens of the invariant residues and the side chain of Ser124. Ser124 is located on the back of the active site among a number of other conserved residues, opposite to the NAD⁺ binding pocket. The equivalent residues in Met8p and CysG are largely glycines and prolines and so it had originally been proposed that these residues would be involved in domain motions or substrate binding [15]. A Ser124Ala variant was found to have 33% of the wild type activity, supporting a role of Ser124 in substrate binding and maximizing enzyme activity (Table 2). In our apoenzyme crystal structure, Ser124 points away from the active site, although a minor conformational change upon substrate binding might induce it to face the active site.

A side chain extending from position 127 would protrude into the cleft suggesting that invariant Gly127 may have been selected not only to facilitate a turn in secondary structure, but also to permit tight interactions with the substrate. The hydroxyl side chain of Ser129 points away from the active site and forms a hydrogen bond with the amide nitrogen of Ile132. This linkage may support the tight turn between strand-8 and helix-5. The adjacent Pro130 sits slightly above the B-ring of the tetrapyrrole-derived substrate and may contribute both a structural role in the initiation of helix-5 and hydrophobic interactions with the B-ring. Arg159 enters the active site near Pro130 and potentially contributes both hydrogen bonds and a compensatory positive charge to the precorrin-2 carboxylates, potentially the C-ring acetate.

A phosphorylated serine residue was identified in the structure of CysG at position Ser128 [22]. This residue is equivalent to Thr125 in SirC and, intriguingly, SirC electron density that we interpret as a free sulfate group is apparently adjacent to Thr125 at the same position as the phospho-group in CysG. A regulatory role for CysG phosphorylation was proposed based on the observation that mutation of Ser128 to Ala resulted in a variant that was fully active whereas mutation to Asp was inhibitory [22]. The sulfate moiety found in the SirC structure is one of many sulfates modelled in the structure due to the high concentration of ammonium

sulfate in the crystallization solution. There is no evidence for a covalent interaction as would be expected if the threonine was actually phosphorylated in our structure, and the hydrogen bond distance between a sulfate oxygen and the Thr125 hydroxyl is 2.6 Å. The presence of the ion in both structures suggests a readiness of this pocket on the surface of the protein to accept negatively charged ions such as the precorrin-2 carboxylates, and further substantiates a role for this pocket in binding the substrate.

Characterization of other active site residues. The Met8p active site includes Asp141, which has been proposed to function as a general base for catalysis [15]. Interestingly, SirC displays a serine (Ser101) at the equivalent position, although there is a nearby aspartate (Asp105) displaced by ~6 Å from the equivalent Met8p site. These residues, and the intervening Ser102 residue whose density is poorly defined, were investigated by mutagenesis. Surprisingly, mutation of either serine to alanine resulted in a 1.4 (Ser101Ala) and 2.3 (Ser102Ala) fold increase in activity (Table 2),

Guided by the Met8p structure and the importance of Met8p Asp141 for metal chelation [15], SirC Ser101 was changed to Asp to see if this generated a protein that had chelatase activity. Although this variant did not display any metal inserting activity, the SirC Ser101Asp protein did display enhanced dehydrogenase activity (Table 2). Interestingly, mutation of Asp105 to Ala also resulted in an increase in activity of SirC (Table 2), demonstrating that this residue does not have an essential role in catalysis and that SirC Asp105 is not equivalent to Met8p Asp141.

These studies indicate that the SirC active site does not house a conserved nucleophile that is used to help promote the dehydrogenation, and we favour a model in which catalysis results from the proximity of the tetrapyrrole-derived substrate with bound NAD⁺. Surprisingly, many of the mutant variants had increased catalytic activity in comparison to wild type SirC. In part, this may be due to the instability of the wild type enzyme, which has a tendency to aggregate over time. It may be that the various mutations enhanced the stability of the enzyme, permitting a higher apparent activity. Without an accurate active site titrant it is not possible to make further comment. It would have been useful to have characterized many of the mutants made in this study further, especially with respect to K_m and k_{cat} values. However, the difficulty of making the precorrin-2 substrate and performing the assays under strict anaerobic conditions precluded the generation of such data.

Metal binding studies of Met8p and SirC from *B. megaterium*. It is a logical assumption to make that the chelatase activity of Met8p is likely to have evolved by acquisition of metal binding ability within a protein such as SirC. With this in mind we thought that it may be possible to identify how the metal ion that is required for ferrochelation activity is bound in Met8p by comparing it to SirC. However, neither sequence alignments nor crystal soaks indicated a conserved metal binding site in Met8p. We thus thought that it may be possible to identify a metal binding site in Met8p by electron paramagnetic resonance (EPR) and distinguish some of the ligands involved.

Met8p was subject to EPR spectroscopy in the presence of either Co(II) or Cu(II) because it is known to possess cobaltochelate activity during anaerobic cobalamin biosynthesis [14] and because Cu(II) can often substitute for Co(II) and has a more readily interpretable EPR spectrum. Co(II) and Cu(II) EPR spectra are sensitive reporters of the ion environment because the spin and orbital energies of the ion's unpaired electrons are affected by the arrangement and nature of the atoms ligating the ion. SirC from *B. megaterium* was

originally deployed as a negative control in these studies, but surprisingly it became apparent that SirC was also able to bind both Co(II) and Cu(II) in the same configuration as seen for Met8p.

The Cu(II) EPR spectra (Figure 5) are clearly different in the presence, a), and absence, c), of stoichiometric SirC. Cu(II) EPR spectra are axial in symmetry, having a large first derivative g_{\perp} feature to high field often overlapping four smaller g_{\parallel} features having absorption line shapes which arise from the hyperfine splitting (A_{\parallel}) of the spectrum by the $I=3/2$ Cu nuclear spin [31]. The single unpaired electron of the Cu(II) ion is located in the dz^2 orbital. Therefore the aforementioned hyperfine splitting and the g_{\parallel} value are indicative of the ligand arrangement around the Cu(II) ion. For Cu(II) bound to SirC these values are $g_{\parallel} = 2.19$ and $A_{\parallel} = 194\text{G}$. However, for Cu(II) ion in the experiment buffer alone, $g_{\parallel} = 2.23$ and $A_{\parallel} = 180\text{G}$, clearly distinguishable from the SirC-bound form. However, in the presence of Met8p, again at a one to one protein to metal ion stoichiometry, the Cu(II) spectrum, Figure 5b, displays identical g_{\parallel} and A_{\parallel} values to those observed in the presence of SirC. These parameters can be interpreted based on knowledge of the EPR parameters of Cu(II) complexes of known structure [32]. They suggest that the Cu(II) binding site on SirC, and Met8p, consists of at least two nitrogen ligands, together with two oxygen ligands. The geometries of these ligating groups are identical in both SirC and Met8p.

Co(II) ions in the high spin state have three unpaired electrons ($S = 3/2$) and consequently give rise to a broad signal at high g value ($g = 5.8$) with unresolved hyperfine splitting [31]. This makes such spectra difficult to analyse, but small qualitative differences are evident in linewidth and g value on binding Co(II) to SirC, Figure 6. This suggests that SirC is also able to bind to a metal ion that is a known substrate for Met8p, i.e. Co(II). An octahedral environment containing several strong ligands such as nitrogens would be expected to effect a spin state change in the Co(II) ion, leading to pairing of some electrons and a large change in the spectrum (including a change in g value to below $g = 3$) [31]. Since Figure 6 shows no evidence of such a change, the Co(II)/Cu(II) binding site on SirC is probably tetrahedral or tetragonal and includes no more than two nitrogens.

Both spectra illustrate that SirC binds metal ions with the same geometry and type of ligands as Met8p. It is not possible to establish which residues are responsible for metal binding using sequence and structural comparisons because there is insufficient sequence conservation and structural similarities. Thus, rather than Met8p being an enzyme that has acquired metal binding and chelation activity, it seems more likely that SirC is an enzyme that has lost its chelation activity.

In summary, we have solved the crystal structure of the *B. megaterium* precorrin-2 dehydrogenase (SirC) and shown that it has a very similar structure to that of Met8p and the N-terminal region of CysG. Mutagenesis studies have revealed that the enzyme does not appear to have a residue within the active site that acts as a general base during the catalytic cycle of the enzyme. Indeed, individually changing a number of residues generated enzymes that have significantly more activity than the wild type enzyme. For biosynthetic enzymes involved in the synthesis of small quantities of natural products such as siroheme and vitamin B₁₂, there is no pressing reason for them to be highly active. Unexpectedly, SirC was found to bind metal ions such as Co(II) and Cu(II) in the same manner as Met8p, which is required to bind metal for its chelatase activity. This may reflect the evolutionary history of SirC as a bifunctional enzyme that has lost an earlier chelatase activity. The proposed loss of ferrochelation activity in SirC results in production of the sirohydrochlorin product, which

Structure of a precorrin-2 dehydrogenase

can be acted upon by specific ferro- and cobaltochelatas for transformation into either siroheme or cobalamin.

Stage 2(a) POST-PRINT

THIS IS NOT THE FINAL VERSION - see doi:10.1042/BJ20080785

ACKNOWLEDGEMENTS.

The research was supported by a grant from the Biotechnology and Biological Sciences Research Council (BBSRC) and from NIH RO1 GM56775 and P30 DK072437. Protein coordinates and structure factor amplitudes have been submitted to the protein databank with PDB code: 3DFZ.

Stage 2(a) POST-PRINT

REFERENCES

- 1 Murphy, M. J. and Siegel, L. M. (1973) Siroheme and sirohydrochlorin. The basis for a new type of porphyrin-related prosthetic group common to both assimilatory and dissimilatory sulfite reductases. *J. Biol. Chem.* **248**, 6911-6919
- 2 Murphy, M. J., Siegel, L. M., Tove, S. R. and Kamin, H. (1974) Siroheme: a new prosthetic group participating in six-electron reduction reactions catalyzed by both sulfite and nitrite reductases. *Proc. Natl. Acad. Sci. U S A.* **71**, 612-616
- 3 Vega, J. M. and Garrett, R. H. (1975) Siroheme: a prosthetic group of the *Neurospora crassa* assimilatory nitrite reductase. *J Biol. Chem.* **250**, 7980-7989
- 4 Crane, B. R. and Getzoff, E. D. (1996) The relationship between structure and function for the sulfite reductases. *Curr. Opin. Struct. Biol.* **6**, 744-756
- 5 Leech, H. K., Raux-Deery, E., Heathcote, P. and Warren, M. J. (2002) Production of cobalamin and sirohaem in *Bacillus megaterium*: an investigation into the role of the branchpoint chelatases sirohydrochlorin ferrochelatase (SirB) and sirohydrochlorin cobalt chelatase (CbiX). *Biochem. Soc. Trans.* **30**, 610-613
- 6 Schubert, H. L., Raux, E., Warren, M. J. and Wilson, K. S. (2001) Optimization of Met8p crystals through protein-storage buffer manipulation. *Acta Crystallogr. D Biol. Crystallogr.* **57**, 867-869
- 7 Johansson, P. and Hederstedt, L. (1999) Organization of genes for tetrapyrrole biosynthesis in gram-positive bacteria. *Microbiology* **145**, 529-538
- 8 Raux, E., Leech, H. K., Beck, R., Schubert, H. L., Santander, P. J., Roessner, C. A., Scott, A. I., Martens, J. H., Jahn, D., Thermes, C., Rambach, A. and Warren, M. J. (2003) Identification and functional analysis of enzymes required for precorrin-2 dehydrogenation and metal ion insertion in the biosynthesis of sirohaem and cobalamin in *Bacillus megaterium*. *Biochem. J.* **370**, 505-516
- 9 Warren, M. J., Stolorow, N. J., Santander, P. J., Roessner, C. A., Sowa, B. A. and Scott, A. I. (1990) Enzymatic synthesis of dihydrosirohydrochlorin (precorrin-2) and of a novel pyrrocorphin by uroporphyrinogen III methylase. *FEBS Lett.* **261**, 76-80
- 10 Schubert, H. L., Raux, E., Wilson, K. S. and Warren, M. J. (1999) Common chelatase design in the branched tetrapyrrole pathways of heme and anaerobic cobalamin synthesis. *Biochemistry* **38**, 10660-10669
- 11 Raux, E., Thermes, C., Heathcote, P., Rambach, A. and Warren, M. J. (1997) A role for *Salmonella typhimurium* cbiK in cobalamin (vitamin B₁₂) and siroheme biosynthesis. *J Bacteriol.* **179**, 3202-3212
- 12 Brindley, A. A., Raux, E., Leech, H. K., Schubert, H. L. and Warren, M. J. (2003) A story of chelatase evolution: identification and characterization of a small 13-15 kDa "ancestral" cobaltochelatase (CbiXS) in the archaea. *J. Biol. Chem.* **278**, 22388-22395
- 13 Hansen, J., Muldbjerg, M., Cherest, H. and Surdin-Kerjan, Y. (1997) Siroheme biosynthesis in *Saccharomyces cerevisiae* requires the products of both the MET1 and MET8 genes. *FEBS Lett.* **401**, 20-24
- 14 Raux, E., McVeigh, T., Peters, S. E., Leustek, T. and Warren, M. J. (1999) The role of *Saccharomyces cerevisiae* Met1p and Met8p in sirohaem and cobalamin biosynthesis. *Biochem. J.* **338**, 701-708
- 15 Schubert, H. L., Raux, E., Brindley, A. A., Leech, H. K., Wilson, K. S., Hill, C. P. and Warren, M. J. (2002) The structure of *Saccharomyces cerevisiae* Met8p, a bifunctional dehydrogenase and ferrochelatase. *EMBO J.* **21**, 2068-2075
- 16 Yin, J., Xu, L. X., Cherney, M. M., Raux-Deery, E., Brindley, A. A., Savchenko, A., Walker, J. R., Cuff, M. E., Warren, M. J. and James, M. N. (2006) Crystal structure of the vitamin B₁₂ biosynthetic cobaltochelatase, CbiX^S, from *Archaeoglobus fulgidus*. *J Struct Funct Genomics.* **7**, 37-50

- 17 Al-Karadaghi, S., Hansson, M., Nikonov, S., Jönsson, B. and Hederstedt, L. (1997) Crystal structure of ferrochelatase: the terminal enzyme in heme biosynthesis. *Structure* **5**, 1501-1510
- 18 Schubert, H. L., Raux, E., Matthews, M. A., Phillips, J. D., Wilson, K. S., Hill, C. P. and Warren, M. J. (2002) Structural diversity in metal ion chelation and the structure of uroporphyrinogen III synthase. *Biochem. Soc. Trans.* **30**, 595-600
- 19 Spencer, J. B., Stolowich, N. J., Roessner, C. A. and Scott, A. I. (1993) The *Escherichia coli* *cysG* gene encodes the multifunctional protein, siroheme synthase. *FEBS Lett.* **335**, 57-60
- 20 Warren, M. J., Roessner, C. A., Santander, P. J. and Scott, A. I. (1990) The *Escherichia coli* *cysG* gene encodes S-adenosylmethionine-dependent uroporphyrinogen III methylase. *Biochem. J.* **265**, 725-729
- 21 Warren, M. J., Bolt, E. L., Roessner, C. A., Scott, A. I., Spencer, J. B. and Woodcock, S. C. (1994) Gene dissection demonstrates that the *Escherichia coli* *cysG* gene encodes a multifunctional protein. *Biochem. J.* **302**, 837-844
- 22 Stroupe, M. E., Leech, H. K., Daniels, D. S., Warren, M. J. and Getzoff, E. D. (2003) CysG structure reveals tetrapyrrole-binding features and novel regulation of siroheme biosynthesis. *Nat. Struct. Biol.* **10**, 1064-1073
- 23 Otwinowski, Z. (1993) Oscillation data reduction program. In *Data Collection and Processing*. (Sawyer, L., Isaacs N. and Bailey, S., eds.), SERC Daresbury, Warrington, UK
- 24 Terwilliger, T. C. and Berendzen, J. (1999) Automated MAD and MIR structure solution. *Acta Crystallogr. Sect. D Biol. Crystallogr.* **55**, 849-861
- 25 Terwilliger, T. C. (2000) Maximum-likelihood density modification. *Acta Crystallogr. Sect. D Biol. Crystallogr.* **56**, 965-972
- 26 Jones, T. A., Zou, J. Y., Cowan, S. W. and Kjeldgaard, M. (1991) Improved Methods for Building Protein Models in Electron-Density Maps and the Location of Errors in These Models. *Acta Crystallogr. Sect. A Found. Crystallogr.* **47**, 110-119
- 27 Emsley, P. and Cowtan, K. (2004) Coot: model-building tools for molecular graphics. *Acta Crystallogr. Sect. D Biol. Crystallogr.* **60**, 2126-2132
- 28 Bailey, S. (1994) The Ccp4 Suite - Programs for Protein Crystallography. *Acta Crystallogr. Sect. D Biol. Crystallogr.* **50**, 760-763
- 29 Murshudov, G. N., Vagin, A. A. and Dodson, E. J. (1997) Refinement of macromolecular structures by the maximum-likelihood method. *Acta Crystallogr. Sect. D Biol. Crystallogr.* **53**, 240-255
- 30 Lesk, A. M. (1995) NAD-binding domains of dehydrogenases. *Curr. Opin. Struct. Biol.* **5**, 775-783
- 31 Mabbs, F. E. and Collison, D. (1992) *Electron Paramagnetic Resonance of d Transition Metal Compounds*. Elsevier, Amsterdam
- 32 Peisach, J. and Blumberg, W. E. (1974) Structural implications derived from the analysis of electron paramagnetic resonance spectra of natural and artificial copper proteins. *Arch. Biochem. Biophys.* **165**, 691-708

Table 1. Data collection and refinement statistics

Space Group H32	Native	KCl ₄ Pt	Thimerisol	
Unit cell	a=b= c=	108.6 201.03	108.6 200.7	108.7 199.9
Number observations	192283	58434	175874	
Number of unique reflections	20508	18841	30506	
Resolution range (Å)	25 – 2.3 (2.38 – 2.3)	20 – 2.9 (3.0 – 2.9)	20 – 2.5 (2.59 – 2.5)	
Completeness (%)	99.4 (94.7)	96.3 (99.2)	99.7 (98.5)	
I/sigma(I)	35.6 (5.4)	6.6 (1.2)	23.3 (6.9)	
Rsym ¹	6.2 (35.2)	16.8 (42.7)	7.2 (25.9)	
Rfactor ² (run56)	19.5			
Rfree	26.3			
rmsd bonds (Å)	0.013			
angles (°)	1.42			
 main chain	43.9			
side chain	44.6			
waters	42.2			
Ligands:SO4 (7) GOL (1)	57.9			

¹Rsym = 100 x $\sum |I - \langle I \rangle| / \sum I$, where $\langle I \rangle$ is the average intensity from multiple observations of symmetry related reflections.

²Rcyst = 100 x $\sum ||F_o| - |F_c|| / \sum |F_o|$ over 95% of the data. Rfree = Rcrist on 5% of the data not used in refinement.

Table 2. Activities of SirC and protein variants.

Enzyme form	Specific dehydrogenase activity (nmol/min/mg)	% wild type activity
Wild type	20.98 (\pm 2.10)	100
Asn98Ala	4.98 (\pm 1.39)	23.7
Ser101Ala	30.10 (\pm 1.87)	143.5
Ser101Asp	58.55 (\pm 7.42)	279.1
Ser102Ala	48.77 (\pm 3.48)	232.5
Asp105Ala	66.84 (\pm 7.43)	318.6
Ser124Ala	6.92 (\pm 1.40)	33.0

Stage 2(a) POST-PRINT

Figure Legends.

Figure 1. Transformation of uroporphyrinogen III into siroheme and cobalamin. For siroheme synthesis, three steps are involved. Firstly, uroporphyrinogen III is methylated at positions 2 and 7 to yield precorrin-2, then this is oxidised to give sirohydrochlorin and finally iron insertion yields siroheme. These steps are either catalysed by individual enzymes (eg SirA, B and C, as depicted by the three arrows), or by two enzymes (eg Met1p and Met8p, as depicted by the two arrows) or by a single multifunctional enzyme (eg CysG, the one large arrow). In the structures, A = acetate side chain and P = propionate side chain.

Figure 2. Structure of SirC. A) front view of the SirC homodimer, with the three structural domains highlighted; NAD⁺-binding domain (green/light green), central dimerization domain (blue/light blue), and C-terminal helical domain (purple/light purple). B) SirC homodimer viewed from the top looking down on NAD⁺-binding domain with C-terminal helical domains below. C) Structure and sequence based alignment of SirC, Met8p and the N-terminal part of CysG. SirC secondary structure is mapped to the sequence. Invariant residues, between these three sequences and a larger assortment of SirC precorrin-2 dehydrogenases, including: *Staphylococcus aureus* (YP_042039.1), *Geobacillus kaustophilus* (YP_146257.1), *Bacillus cereus* (NP_977872.1), *Bacillus anthracis* (NP_843903.1), *Staphylococcus epidermidis* (NP_765732.1), *Oceanobacillus iheyensis* (NP_692578.1), *Pelotomaculum thermopropionicum* (GAA01341.1), *Heliobacillus mobilis* (ABH04863.1), *Desulfotomaculum reducens* (ZP_01148319.1), *Bacillus halodurans* (NP_242363.1), *Bacillus licheniformis* (YP_078957.1), delta proteobacterium MLMS-1 (ZP_01287446.1), *Moorella thermoacetica* (YP_430108.1) and *Herpetosiphon aurantiacus* (ZP_01424816.1) are boxed in red.

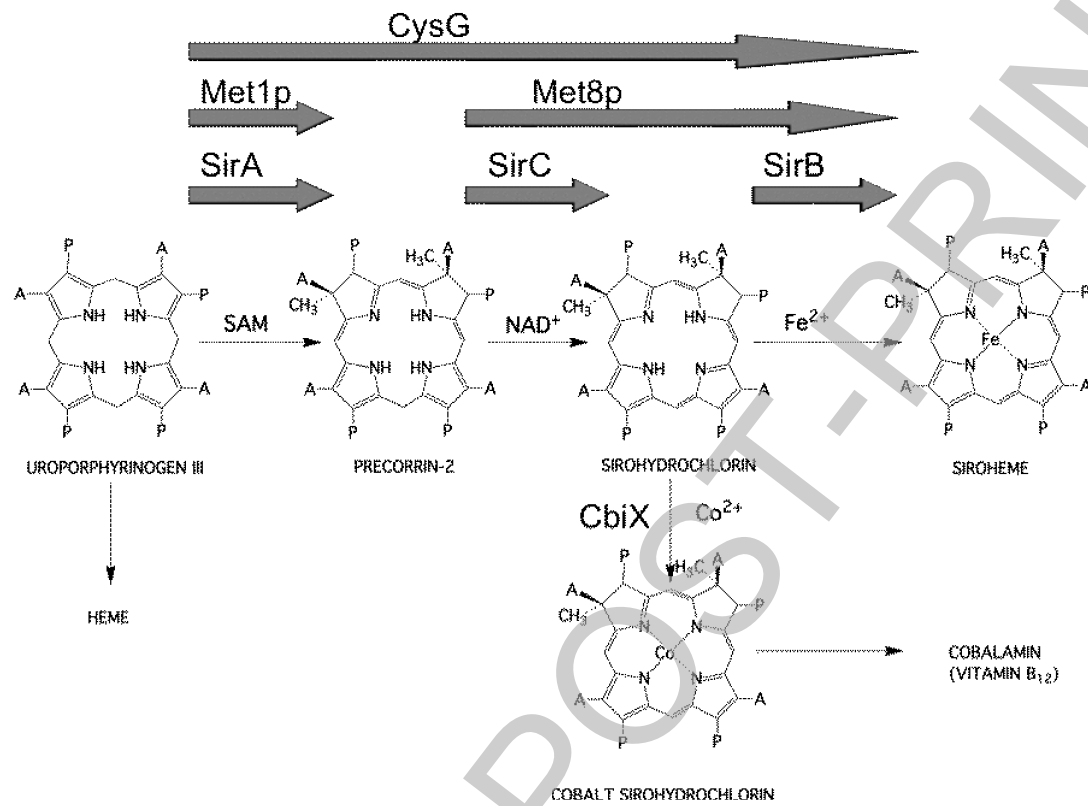
Figure 3. Conformational variation in SirC homologs. A) Alignment of three structures (monomers) based on their NAD⁺-binding domains, SirC (yellow), Met8p (puce), and CysG (orange). SirC active site residues are shown in stick representation. The residues equivalent to SirC Arg159 appear above the active site because they are presented by the other molecule of the homodimer (not shown). Using this alignment, the C-terminal helical domains (bold colour) and central dimerization domains (light colour) are as viewed from the bottom of the structure. B) SirC. C) CysG. D) Met8p.

Figure 4. Stereo-diagram of the SirC active site and putative substrate binding location of precorrin-2 and β -nicotinamide binding sites. Conserved and invariant residues are highlighted. Arg159 is presented from the alternate monomer of the SirC homodimer. The location of the bound SO₄²⁻ group in the SirC structure, and the phosphorylated threonine in the CysG structure is just above the C-ring near Gly127 and Ser124. β -nicotinamide (cyan), SirC (green)

Figure 5. X-band EPR spectra of Cu(II) a) in a 1:1 stoichiometry with SirC, b) in a 1:1 stoichiometry with Met8p, c) in buffer alone. Microwave power 0.5mW, modulation amplitude 5 G for a) and c), 8 G for b), temperature 20 K.

Figure 6. X-band EPR spectra of Co(II) bound to SirC (black line) and free in buffer solution (grey line). Microwave power 0.5 mW, modulation amplitude 5 G, temperature 20 K.

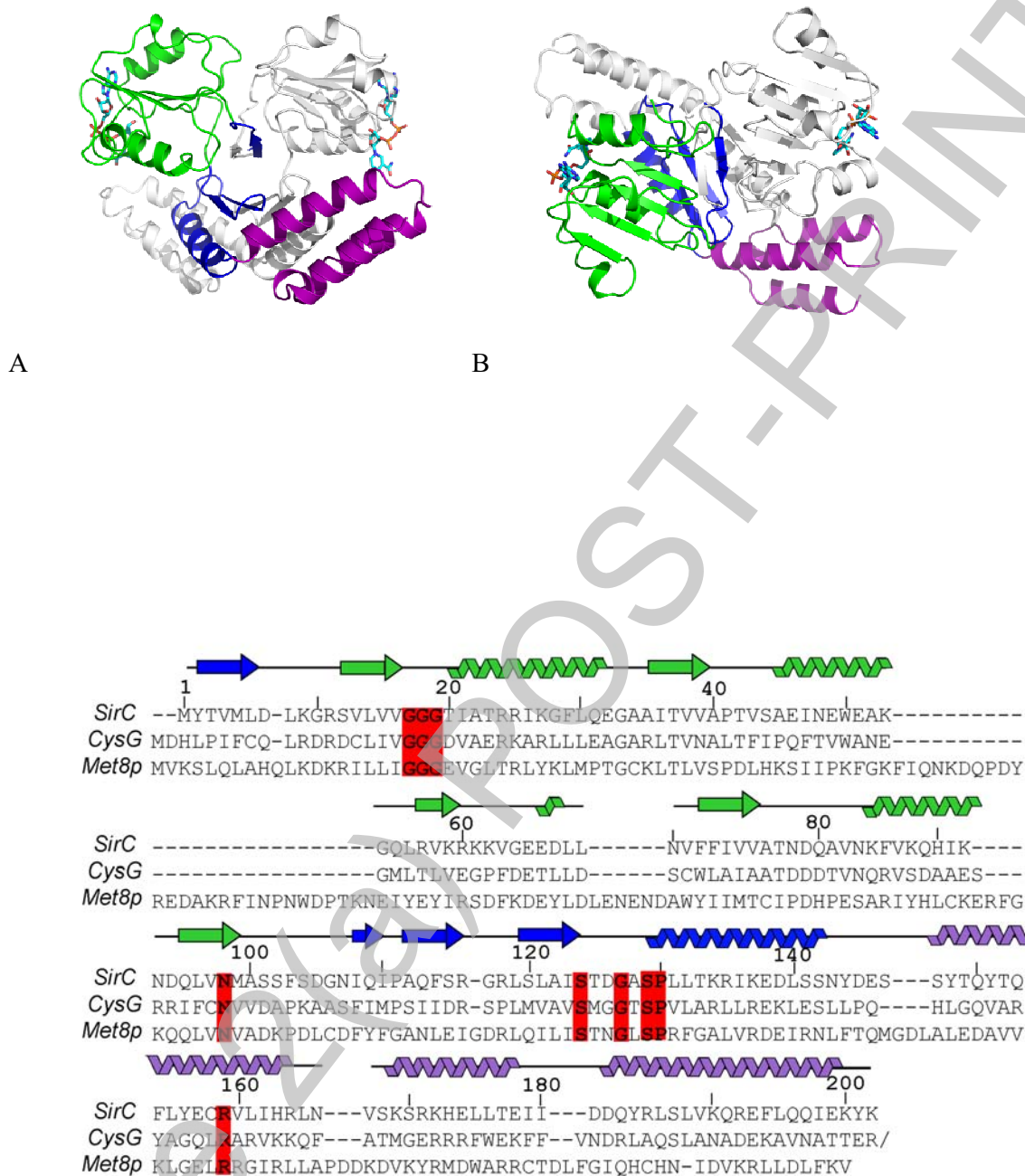
Figure 1



THIS IS NOT THE FINAL VERSION - see doi:10.1042/BJ20080785

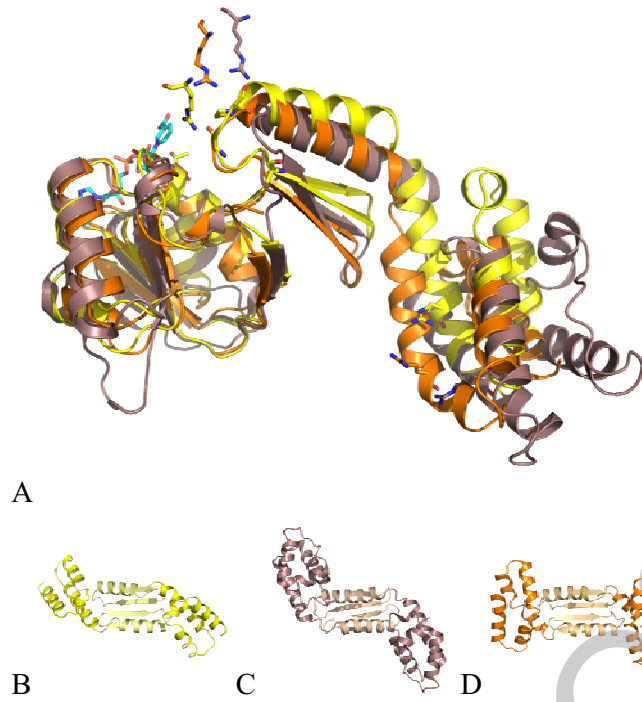
Structure of a precorrin-2 dehydrogenase

Figure 2.



THIS IS NOT THE FINAL VERSION - see doi:10.1042/BJ20080785

Figure 3.



THIS IS NOT THE FINAL VERSION - see doi:10.1042/BJ20080785

Stage 2(a) POST-PRINT

Figure 4

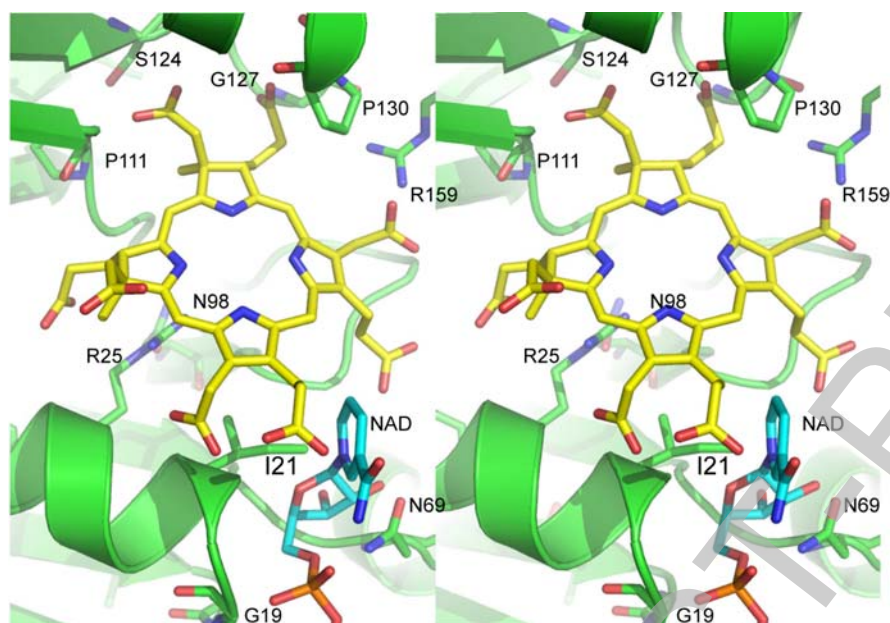
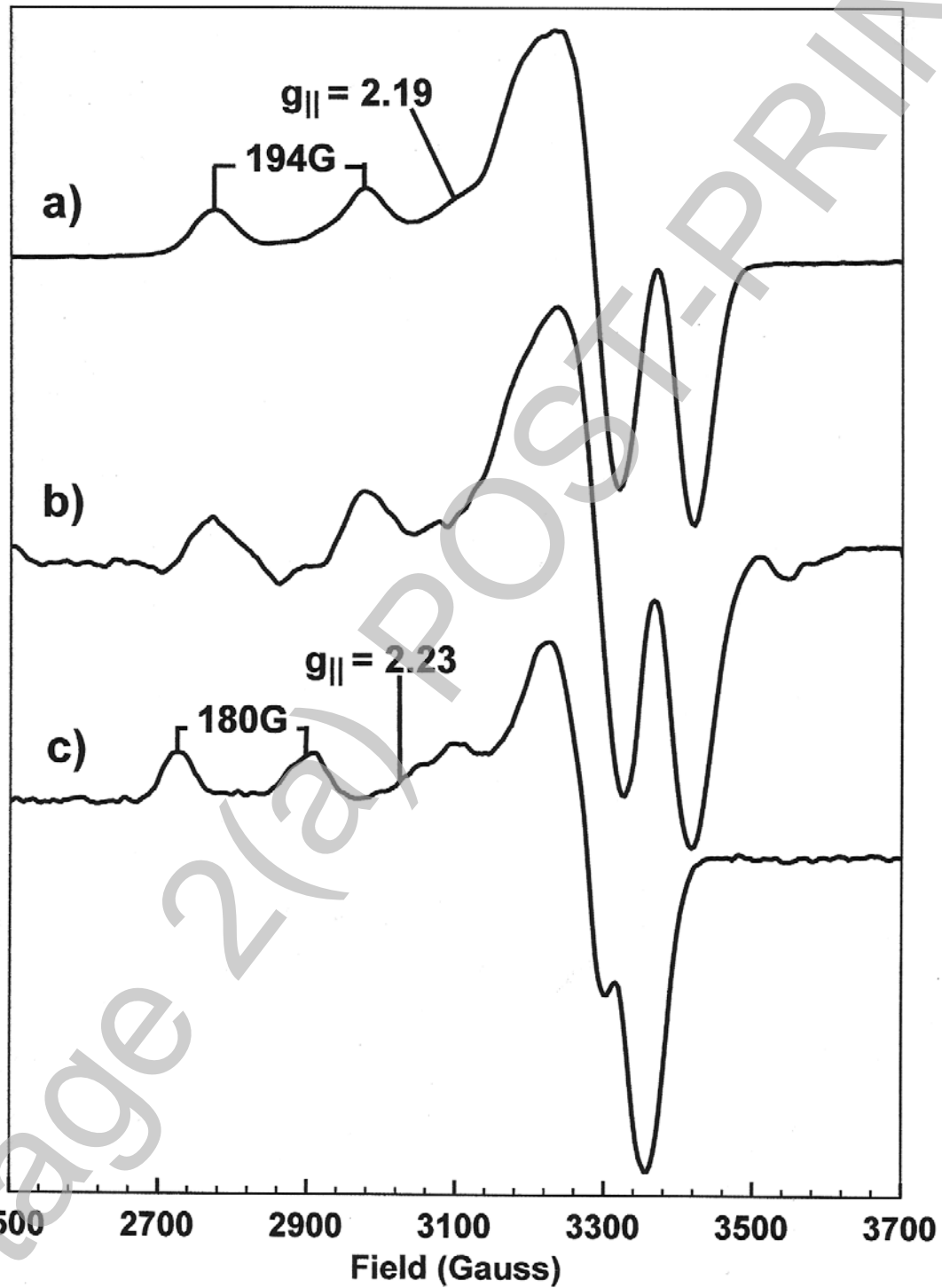


Figure 5



THIS IS NOT THE FINAL VERSION - see doi:10.1042/BJ20080785

Figure 6.

